



Budapest University of Technology and Economics
Faculty of Civil Engineering
Department of Structural Mechanics

Wind load analysis of some typical membrane structures by experimental and numerical approaches

by

Sherly Pool Blanco

Thesis Booklet

Supervised by

Dr. Krisztián Hincz

Budapest, Hungary, 2025

1 Introduction

Tensile membrane structures are lightweight, economical, and environmentally friendly structures with unique and exciting shapes. Their construction is based on a very thin coated membrane, typically less than 1 mm thick, with negligible bending stiffness. Consequently, the loads are transferred solely to the supporting structural elements through tension. They represent an efficient solution for covering large areas with minimal internal support.

The classification of membrane structures is based on their pretension system, which can be categorized into external forces acting along the boundaries and at the supports (tensile membrane structures) or internal overpressure (inflated structures). Tensile structures comprise arches, masts, rings, or cables and the fabric coat. Internally pressurized structures are further divided into two subcategories: air-supported and air-inflated structures. Air-supported structures are fully enclosed and rely on internal air pressure to maintain their shape, while air-inflated structures consist of inflated walls that provide and support their form [1-6]. Figure 1.1 depicts the membrane structure classifications.

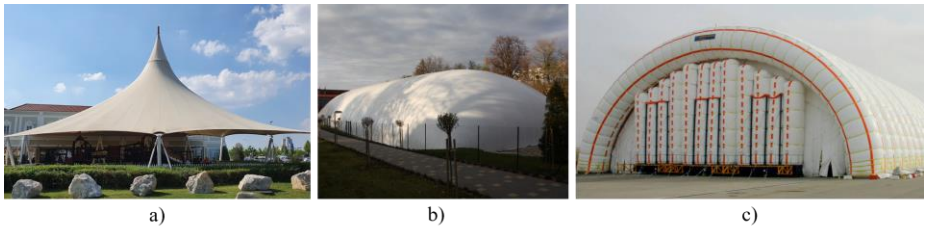


Figure 1.1 Membrane structures classification: a) tensile membrane structures; b) air-supported structures; and c) air-inflated structures

1.1 Analysis of membrane structures

The design and analysis of membrane structures involve different steps compared to conventional structures made of concrete or steel; for example, the shape of these structures cannot be chosen arbitrarily. The geometry, the derived forces, and displacements are determined through an iterative process combining design and structural analysis. As a result, the shape of these structures cannot be chosen arbitrarily.

The analysis of wind load on tensile membrane structures is a crucial issue. One of the most important steps is to compare the maximum membrane stresses caused by wind load with the tensile strength of the membrane material. Furthermore, slack areas and displacements must be evaluated to prevent undesirable fluttering, potentially leading to structural collapse.

1.2 Wind pressure on membrane structures

One of the main challenges in wind analysis is determining the pressure coefficients for doubly curved membranes. Existing design codes do not provide these coefficients for complex hyperbolic and elliptic shapes, so they must be estimated through numerical approximations (Computational Wind Engineering, CWE) or Wind Tunnel tests (WT). In wind tunnels, the pressure coefficients of tensile membrane structures are typically measured using rigid models. However, some studies have highlighted the importance of considering membrane deformations [7].

The wind loads on structures can be quantified using dimensionless parameters known as Pressure Coefficients (C_p). These coefficients depend on the structure's geometry and define the relationship between inertial and viscous forces, as expressed in Equation 1.1.

$$C_p = \frac{p - p_0}{\frac{1}{2}\rho U^2} \quad (1.1)$$

where p is the pressure at a specific point, p_0 is the free upstream pressure, U is the free upstream velocity, and ρ is the fluid density.

Wind tunnel experiments

Wind tunnel tests are applicable when tandards do not provide wind load information. The primary purpose of these tests is to evaluate the reliability and cost-effectiveness of structures. They are also essential for analysing buildings very susceptible to wind loads. Sometimes, wind tunnel analysis is required for buildings with unusual aerodynamic shapes. Various parameters, including pressure, forces, moments, and accelerations, can be measured on scaled models and applied to full-size structures [8].

Computational wind engineering

The CWE is a subfield of Computational Fluid Dynamics (CFD) that focuses on the impact of wind on buildings [9]. This methodology involves solving the differential equations that describe the fluid within a specific domain and under certain boundary conditions. The governing equations for the flow are based on the principles of conservation of mass (continuity) and momentum (Navier-Stokes). In Einstein notation, the continuity equation is represented by Equation 1.2, while the Navier-Stokes equations are defined by Equation 1.3:

$$\frac{\partial U_i}{\partial x_i} = 0 \quad (1.2)$$

$$\frac{\partial U_i}{\partial t} + U_j \frac{\partial U_i}{\partial U_j} = -\frac{1}{\rho} \frac{\partial p}{\partial x_i} + \nu \frac{\partial^2 U_i}{\partial x_j \partial x_j} + f_i \quad (1.3)$$

where U_i is the velocity components in a Cartesian coordinate system ($i = 1, 2, 3$); p is the pressure; ν is the fluid kinematic viscosity; and f_i is the vector representing the body forces.

In addition to the flow equation system, the computational methodology requires additional parameters to describe the instabilities in the fluid, commonly referred to as turbulence. Turbulence involves the presence of eddy motions, which arise from the velocity fluctuations. Various strategies are available to fully solve or model the turbulent eddy motions within the flow, and these strategies differ in computational time and effort.

1.3 Research purpose

The current research aimed to determine the wind load distribution acting on some typical, frequently used membrane structure forms with various structural systems. The study focused on numerical CFD simulations based on steady-state analysis (RANS equations) and experimental wind tunnel measurements. On the one hand, the research tried to answer the question of the reliability of the CFD-based structural analysis in the case of membrane structures with various shapes. On the other hand, the study aimed to determine the wind load distribution on the surface of various membrane structures in the case of different wind directions to support the design of such structures.

The difference between the two approaches (experimental and numerical) can be interpreted in the distribution and magnitude of the wind pressure coefficients. Still, the differences in the membrane forces and displacements calculated based on the experimental and CFD-based pressure distributions are even more interesting.

The adopted methodology was considered to begin with determining the mean pressure coefficient fields over the surface of the membrane structures (experimentally and/or numerically). Then, using numerical methods, these pressure coefficients were applied as part of the external load action in a structural model to compute the membrane forces in the deformed configuration.

The structural analysis was completed with the method developed by Hincz [10]. The geometrically nonlinear numerical method is based on the DRM, and an orthotropic, linear elastic material model was applied. Since the method has been previously published in detail, the dissertation does not present the details of the calculation of the membrane forces and displacements.

The significant displacements of membrane structures (compared to structures composed of conventional building materials) justify the wind load analysis of the deformed shapes of the structures. Although this approach does not constitute a fully coupled fluid-structure interaction analysis, similarities/differences between available experimental results are introduced. This reinforced the value of combining numerical and experimental methods as complementary tools for evaluating the structural response of membrane structures.

Since the dynamic effects rarely cause problems in the case of properly prestressed and well-designed membrane structures (with doubly curved shape without flat areas), only static analysis was applied in the study. The slack areas in the membrane or the lack of

double curvature can result in flutter, which in worst cases can destroy the structure, hence these must be avoided by careful planning (formfinding, prestressing method, etc.).

As a detailed explanation, the wind analysis considered three different membrane structures. The first one, a single mast-supported tent, was investigated only numerically in the current research, and its validation was based on former wind tunnel test results (Chapter 2). Mean pressure coefficients, membrane forces and displacements were calculated and compared. The second analysed structure was an air-inflated hangar investigated with (Chapter 3) and without (Chapter 4) side walls. Additionally, the study included a comparison of wind loads on both the unloaded and the deformed shape of the structure, using both experimental and numerical methods. Lastly, the third analysis compiled a set of arch-supported tensile membrane structures with various lengths and numbers of supporting arches (Chapter 5). The wind pressure on models with four, five, and six supporting arches was measured in the wind tunnel and calculated with the help of the CFD method.

2 Computational Wind Engineering of membrane structures

2.1 Mast-supported structure

This chapter describes the numerical simulation over a mast-supported structure. The structure consists of three main sections: 1) the vertical walls, 2) the hyperbolic membrane, and 3) the closing cap at the top (Figure 2.1). Previous wind tunnel experiments provided data such as mean pressure coefficients and displacements [7]. The wind tunnel tests were conducted using a rigid scale model (1:30) containing 132 measurement points, as shown in Figure 2.2.

The numerical simulations focused on the determination of pressure coefficient maps based on steady-state analyses with $k\varepsilon R$ and $k\omega SST$ turbulence models. According to [11-13], it is recommended that the dimensions of the domain should extend at least $5H$ from the structure's surface to the inlet, lateral, and top boundaries, where H represents the structure's height. Additionally, the distance from the structure's walls to the outlet surface should be at least $15H$.

Results compared mean pressure coefficients, membrane forces and displacements, and strain energy.

In summary, both turbulence models offered a qualitatively good approximation of the pressure results based on wind tunnel tests. However, notable differences were observed in areas significantly affected by flow separation. Finally, the largest difference in the membrane forces and maximum displacements were 20% and 12%, respectively.

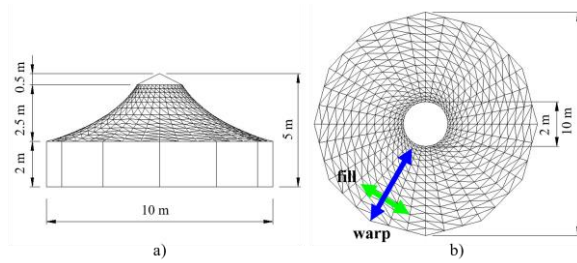


Figure 2.1 Mast-supported structure. Prototype dimensions: a) front and b) top views



Figure 2.2 Mast-supported structure (rigid scale model with measurement points)

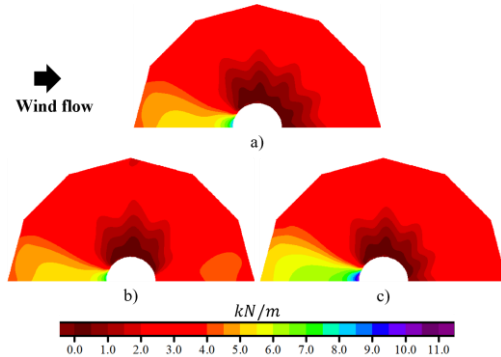


Figure 2.3 Mast-supported structure. Membrane forces based on the wind pressure values from a) WT tests, b) $k\varepsilon R$ and c) $k\omega SST$ turbulence model

3 Air-inflated structure (enclosed and open)

This section introduces the CWE analysis of an air-inflated hangar. The prototype structure consists of six arched tubes of 3 m diameter each. The total length (L) and height (H) of the structure are 13 meters, and its width (W) is 26 meters. In addition, three grid resolutions, four turbulence models, and five wind directions were included in the research.

Mean pressure coefficients measured on a 1:72.5 scale model are reported in [14]. The included wind directions were 0° , 45° , and 90° , and two structure conditions: enclosed and open. Figure 3.1 shows the dimensions of the prototype structure and the analysed wind directions.

In addition to the recommendations cited by [11-13], in the current study, a double inlet/outlet domain was applied. This feature was suitable for analysing various oblique wind directions without re-meshing.

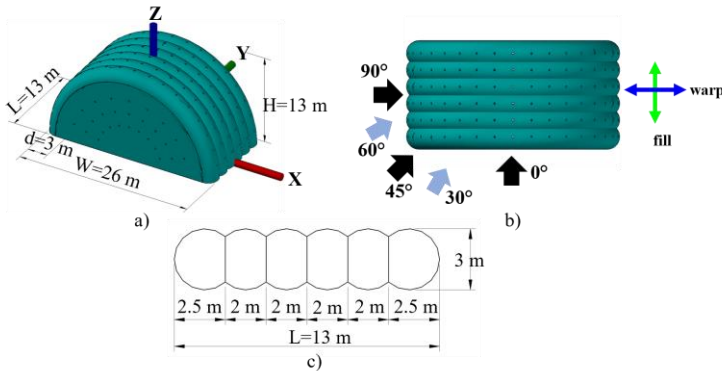


Figure 3.1 Air-inflated structure. a) Prototype dimensions, and b) analysed wind directions

Enclosed condition

Figure 3.2 compares the mean pressure coefficients based on the numerical approximations and results reported by wind tunnel experiments. It also compares the differences between the four turbulence models. Overall, the results from all turbulence models were mostly accurate; however, the most significant differences were observed in areas significantly influenced by additional eddy motions caused by flow separation.

Taking into account the 0° , 45° , and 90° wind directions, the most important mispredictions to the maximum C_p values were 7%, 3%, and 5%, respectively (considering all turbulence models). Nonetheless, the largest mispredictions to the minimum C_p were more considerable: 13%, 68%, and 41% for the three abovementioned wind directions.

In addition to the mean pressure comparison, membrane forces and displacement were examined. Even though mean pressure differences were at some point remarkable, the analysis of the membrane forces and displacements was more promising from a structural point of view. For instance, the most significant WT-based displacement was 1622 mm at the windward side of the structure when the wind direction was 90° . Then, the most considerable difference between the WT and CWE-based solutions was 6%.

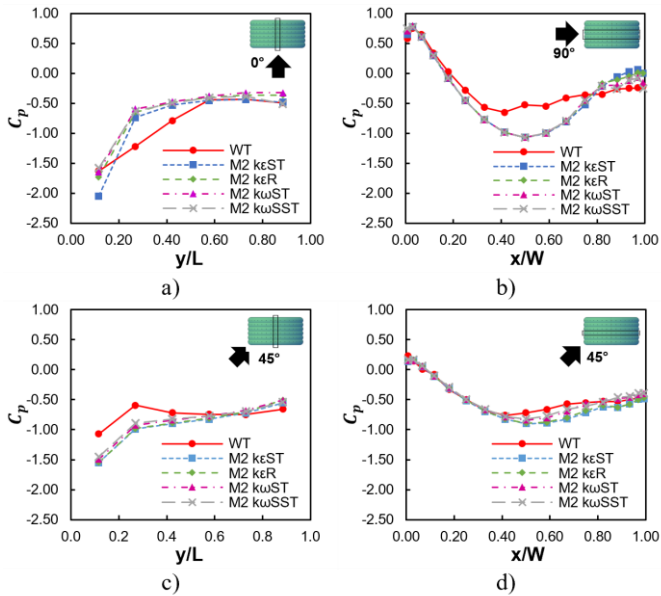


Figure 3.2 Air-inflated structure (enclosed). Pressure coefficients based on the finest grid and different turbulence models: a) 0°, b) 90°, and c-d) 45° wind directions

Open condition

Figure 3.3 depicts the geometry dimensions of the open structure also, the studied wind direction. The following analysis only considered one grid resolution and a unique turbulence model. The domain criteria, boundary conditions, and software settings used in the analysis of the enclosed structure were also applicable to the open case. Table 3.1 summarizes the maximum and minimum pressure coefficients based on former wind tunnel tests and the numerical approximations.

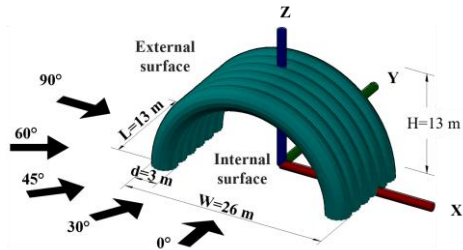


Figure 3.3 Air-inflated structure (open). Computational domain without the top surface (left); membrane surface discretization (right).

Based on the experimental results, the most significant negative C_p on the internal surface was -1.196, which occurred during the 45° wind direction. The numerical simulations overestimated this coefficient by 56%, giving a value of -1.861. In contrast, the estimation of the minimum external C_p by the CWE was approximately 10% higher than the value measured by WT tests (-1.515 compared to -1.388, respectively).

When comparing the largest positive C_p , the CWE analysis provided results for the internal membrane surface that closely matched those from WT tests, showing only a 1% difference (0.705 versus 0.692). However, the CWE estimation of the largest positive C_p on the external surface was 7% higher than the one given by WT tests, with values of 0.785 and 0.731, respectively.

Table 3.1 Air-inflated structure (open). Maximum and minimum C_p based on WT tests and CWE approximations

Wind direction	Surface	WT		CWE	
		Max.	Min.	Max.	Min.
0°	External	-0.297	-1.228	-0.261	-1.139
	Internal	-0.069	-0.794	-0.306	-1.235
30°	External	-	-	0.260	-1.752
	Internal	-	-	0.471	-1.654
45°	External	0.770	-1.388	0.643	-1.515
	Internal	0.692	-1.196	0.705	-1.861
60°	External	-	-	0.782	-1.352
	Internal	-	-	0.785	-2.473
90°	External	0.731	-0.802	0.785	-1.039
	Internal	-0.039	-0.636	0.073	-0.344

Deformed shape

This section introduces the mean pressure distribution of the deformed shape of the air-inflated membrane structure. It was calculated by applying the Dynamic Relaxation Method (DRM) [15, 16] considering the wind impact at 90°. The maximum displacement based on the experimental pressure coefficients was approximately 2.7 m (located at the windward side).

The mean pressure distribution over the deformed shape was measured by WT tests and determined by the CWE methodology (Figure 3.4-3.5). The analysis of the deformed shape showed that the effect of displacements could significantly impact the pressure distribution. Both methods showed that on the external surface of the deformed shape, the positive pressure area was considerably larger than on the undeformed shape.

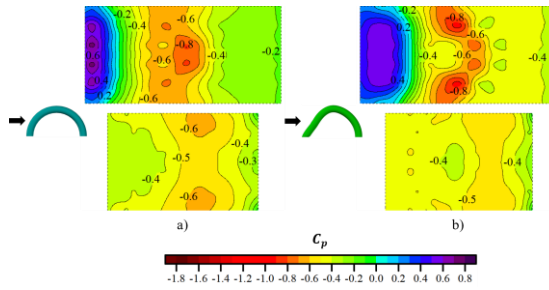


Figure 3.4 Air-inflated structure (open). WT-based pressure coefficients on the external (top) and internal (bottom) membrane surfaces. a) undeformed and b) deformed structure.

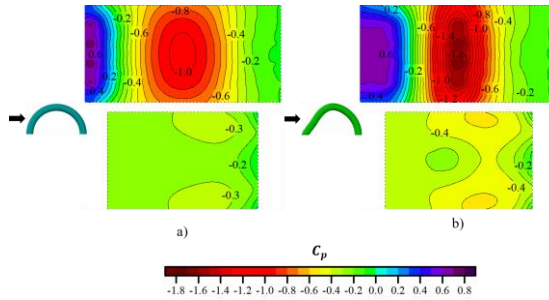


Figure 3.5 Air-inflated structure (open). CWE-based pressure coefficients on the external (top) and internal (bottom) membrane surfaces. a) undeformed and b) deformed structure.

4 Arch-supported structure

The current chapter describes wind tunnel experiments of a series of arch-supported membrane structures. The prototype structures consist of 3, 4, and 5 modules supported by 4, 5, and 6 arches. The structures' height and width are equal to 30 m and 60 m, respectively. Meanwhile, their lengths are 100 m (5-module structure), 80 m (4-module structure), and 60 m (3-module structure). Figure 4.1 depicts the geometry and dimensions of the 5-module structure.

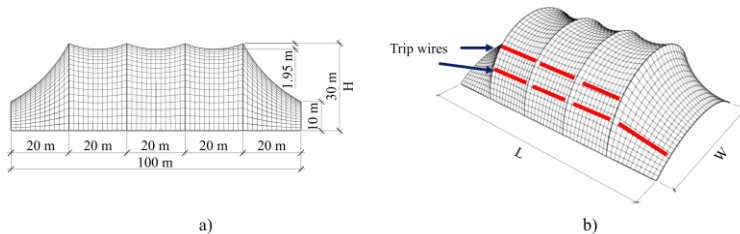


Figure 4.1 Arch-supported structure. 5-module structure: a) top and b) isometric views.

The model was manufactured using a 3D printer with a 1:250 scale. Each module had 36 holes where pressure tap measurements were placed. Thus, the 5-module structure had 180 measurement points, the 4-module had 144, and the 3-module had 108. Figure 4.2 illustrates the scale models.

Eleven wind directions were studied, ranging from 0° to 90° in 10° steps and including the oblique wind direction of 45°. (0° was set perpendicular to the central axis of the structure.)

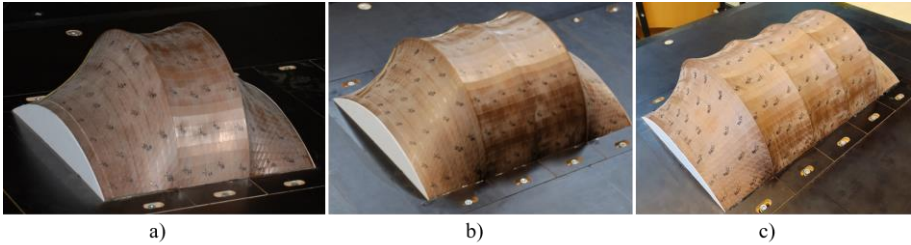


Figure 4.2 Arch-supported structure. Scale models. a) 3-module, b) 4-module, and c) 5-module structure

The measured pressures are summarized in mean pressure coefficient, peak negative, peak positive, and standard deviation pressure coefficient maps. A comparison of mean pressure coefficients on the midline of the 5-module structure with various experimental data and design codes is illustrated in Figure 4.3.

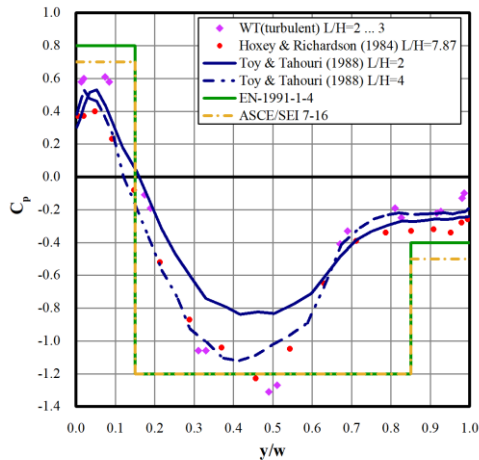


Figure 4.3 Arch-supported structure. Pressure coefficients at the measurement points close to the midline of the 5-module structure at 0° wind direction, comparison between full-size measurements, experimental tests, and design codes

Results showed that the critical wind directions were 40° and 45° , recalling the importance of the wind analysis of the structures under oblique wind directions, which are not usually found in the literature.

The maximum mean pressure coefficient was approximately the same for all structures, which proves that the length dimension has no significant effect on the positive pressure.

In contrast, the variation in the minimum mean pressure coefficient is associated with changes in the length dimension of the structure, and this value increased by the length.

5 New scientific results

The current section summarizes the scientific contributions based on the completed research.

5.1 Thesis 1

I analysed a hyperbolic membrane roof with a regular dodecagon floor plan, vertical walls and a single mast support in the middle of the structure. The height of the structure was 5 m, the length of the longest diagonal of the floor plan was 10 m. I calculated pressure coefficient distributions using a 3D steady-state Computational Fluid Dynamics (CFD) analysis with Reynolds-averaged Navier-Stokes (RANS) strategy and two-equation turbulence models, $k\varepsilon R$ and $k\omega SST$. The numerical simulation was validated with former wind tunnel test results of a 1:30 scale model of the same structure. The analysis with the $k\varepsilon R$ turbulence model was based on the full-size structure, while the $k\omega SST$ turbulence model used a 1:30 scale ratio similar to the wind tunnel tests. The membrane forces and displacements were calculated with a Dynamic Relaxation based method according to the various pressure coefficient distributions.

- Both turbulence models provided a qualitatively good approximation to the Wind Tunnel (WT)-based pressure coefficient distributions; however, significant local differences were found in those areas highly influenced by flow separation.
- The research results show that despite the occasional significant local differences between the CFD-based and WT-based pressure distribution fields, the CFD-based maximum membrane forces and displacements provide a good approximation of the WT-based results for the studied structure. The most significant differences in the maximum membrane forces and maximum displacements were 20% and 12%, respectively.

Related publication: Pool Blanco and Hincz (2022).

5.2 Thesis 2

I conducted a detailed wind analysis of a hemicylindrical membrane structure composed of six air-inflated tubes of 3 m diameters. The total length and height of the prototype structure were 13 m, and its width was 26 m. The overpressure in the inflated tubes was 25 mbar. The research presented an overview of the accuracy of the RANS method using four turbulence models commonly available in most commercial CFD software. The structure was analysed with and without side walls (enclosed versus open). The numerical results were compared with my former WT measurement data of the same structure.

- The CFD-based pressure coefficient distributions showed qualitative agreement with the experimental ones. However, there were significant local differences, primarily in the separation zones.
- In the case of the enclosed model the most significant difference in the maximum and minimum pressure coefficient were 7% and 68%, respectively.
- I calculated and compared membrane forces and displacements with the Dynamic Relaxation Method according to experimental and CFD-based pressure coefficients over the enclosed air-inflated structure. The most significant mispredictions in the maximum membrane forces and the largest displacement were 11 % and 6 %, respectively (considering results of all four applied turbulence models). From this point of view, CFD analysis offers an acceptable approximation of pressure distributions for design purposes.
- Simplified, code-like, area-distributed pressure coefficient maps are provided based on the experimental results, which can be applied in the structural analysis of inflated structures with similar shapes.
- On the other hand, the CFD overestimations of the minimum pressure coefficients on the internal and external membrane surface of the open structure were 56% and 10%, respectively. The misprediction of the maximum pressure coefficients either on the internal and external surfaces was less significant, resulting in 1% for the maximum internal pressure coefficient, and 7% for the maximum external pressure coefficient.

Related publications: Pool Blanco et al. (2018); Hincz et al. (2019); Pool Blanco et al. (2022); Pool Blanco and Hincz (2023); Pool Blanco and Hincz (2024).

5.3 Thesis 3

I presented a length dependence study of closed, hemicylindrical air-inflated structures composed of air-inflated tubes of 3 m diameters based on the RANS method with the $k\epsilon$ Standard turbulence model. In addition to the 13-meter-long structure, which was also

experimentally tested in WT, a nine and a 17-meter-long structure were analysed. The height of the analysed structures was 13 m. The overpressure in the inflated tubes was 25 mbar. I focused only on the orthogonal wind directions, which are parallel and perpendicular to the main axis of the structure (0° and 90°).

- I observed that the length of the structure has no significant effect on the maximum and minimum pressure coefficients when the wind direction is parallel to the longitudinal axis of the structure. The maximum pressure coefficient was the same for the nine, thirteen, and 17-meter-long structures (0.89). Meanwhile, the minimum pressure coefficient was only 2% larger in the case of the 17-meter-long structure compared to the 9-meter-long structure.
- In contrast, for the 90° wind direction, both the maximum and minimum pressure coefficient values increased with the length of the structure. The minimum pressure coefficient for the 13-meter and 17-meter-long structures was approximately 32% and 53% larger, respectively, compared to the 9-meter-long structure. However, the differences in positive pressure values were less significant (less than 7% between the longest and the shortest structure).

Related publications: Pool Blanco et al. (2018); Hincz et al. (2019); Pool Blanco et al. (2022); Pool Blanco and Hincz (2023); Pool Blanco and Hincz (2024).

5.4 Thesis 4

I completed the deformed shape wind analysis of an open, hemicylindrical air-inflated structure composed of six air-inflated tubes of 3 m diameters. The total length and height of the analysed structure were 13 m, meanwhile its width was 26 m. An overpressure equal to 25 mbar was considered in the inflated tubes. The wind load application to obtain the deformed shape was considered perpendicular to the central axis of the structure. The deformed shape of the structure was determined by the Dynamic Relaxation Method according to the pressure coefficients measured on the rigid model of the unloaded structure by wind tunnel test. Then, the pressure distribution was measured on the surface of the 3D-printed deformed shape.

- The results showed that the effect of displacements on the pressure coefficient distribution is essential.
- On the one hand, the extent of the positive pressure region on the windward side of the deformed shape is significantly larger than that on the unloaded shape.
- On the other hand, the minimum pressure coefficient at the top of the structure was almost 17% larger in the case of the deformed shape.

Related publication: Pool Blanco and Hincz (2023).

5.5 Thesis 5

I conducted the wind load analysis of a series of arch-supported membrane structures based on wind tunnel experiments and numerical simulations. The prototype geometries were close to a hemicylindrical shape with vertical end walls. The considered arch-supported structures consisted of 5, 4, and 3 modules supported by 6, 5, and 4 arches. The width and height of the structures were 60 m and 30 m, respectively. Meanwhile, the different lengths were 100 m, 80 m, and 60 m (5, 4, and 3 module structures). I obtained pressure distribution on the structure's surfaces for 11 wind directions at 10-degree steps, plus 45° wind direction. I considered the wind analysis of a scale model in a wind tunnel test and the full-scale structure analysis by numerical simulations. The wind tunnel experiments considered a 1:250 scale ratio. Since for the wind directions parallel or almost parallel to the supporting arches, there was a concern about Reynolds number dependency, I considered the application of trip wires of diameter approximately 0.8 [mm] on the model surface.

I calculated wind pressure distributions using a 3D steady-state Computational Fluid Dynamics (CFD) analysis with Reynolds-averaged Navier-Stokes (RANS) equations and the two-equation turbulence models $k\omega SST$. I presented mean, peak minimum, and peak maximum pressure coefficient maps based on the wind tunnel experiments. Additionally, I calculated the lift coefficients and membrane forces for various wind directions considering the 5-module structure.

- In the midline perpendicular to the main axis of the structure, it was observed that the presence of the trip wires reduced the negative pressure at the top of the model. However, an increment of the negative pressure was observed on the downstream side.
- The length dependence study showed that an increase in the structure's length results in higher suction at the top of the structure, but it has almost no effect on the positive pressure on the windward side of the structure.
- Based on the mean pressure coefficients from available standards, the calculation of membrane forces indicated that the most significant overestimation was approximately 20% compared to the membrane forces obtained from current wind tunnel tests.
- When comparing the membrane force resulting from numerical simulations and the wind tunnel experiments, the most significant overestimation was about 11%.

Related publications: Hincz et al., (2024); Hincz et al., (2025)

6 Research activity

6.1 Journal papers

- Pool-Blanco SJ, Hincz K., “Computational wind engineering of a mast-supported tensile structure,” *Periodica Polytechnica Civil Engineering*, 66(1), pp. 210-219, 2022. <https://doi.org/10.3311/PPci.18656>
- Pool-Blanco SJ, Gamboa-Marrufo M, Hincz K, Domínguez-Sandoval C, “Wind tunnel test of an inflated membrane structure. Two study cases: with and without end-walls,” *Ingeniería Investigación y Tecnología*, 23(2), pp:1-12, 2022. <https://doi.org/10.22201/fi.25940732e.2022.23.2.011>
- Pool-Blanco SJ, Hincz K, “Computational wind analysis of an open air-inflated membrane structure,” *Pollack Periodica*, 2023. <https://doi.org/10.1556/606.2023.00804>
- Pool-Blanco SJ, Hincz K, “Computational wind analysis of a closed air-inflated membrane structure,” *KSCE Journal of Civil Engineering*, 2024. <https://doi.org/10.1007/s12205-024-1505-6>
- Hincz K, Pool-Blanco SJ, Balczó M, “Wind analysis of a multispan arch-supported tensile membrane structure,” *Journal of Wind Engineering and Industrial Aerodynamics*, 265, 106181, 2025. <https://doi.org/10.1016/j.jweia.2025.106181>

6.2 Conference papers

- Pool-Blanco SJ, Gamboa-Marrufo M, Hincz K, "Obtención de la configuración deformada de un hangar inflable a partir de la medición de presiones en túnel de viento", in *Memorias del Congreso Internacional de Investigación Academia Journals Chetumal 2018*, Academia Journals, vol. 10, no. 4, pp. 1942-1947, 2018. (in Spanish)
- Hincz K, Pool Blanco SJ, Gamboa-Marrufo M, "Wind analysis of an air-inflated membrane structure," in: *Form and Force: Proceedings of the 60th Anniversary Symposium of the International Association for Shell and Spatial Structures*, pp. 1193-1199, Barcelona, España. October 2019.
- Hincz K, Pool-Blanco SJ, Rosa RJ, Koren M, Balczó M, “Wind load analysis of a series of arch-supported membrane structures,” in: *Proceedings of the IASS 2024 Symposium Redefining the Art of Structural Design*, Block P, Boller G, DeWolf C, Pauli J, and Kaufmann W, Eds. Zurich, Switzerland, 26-30 August 2024. https://app.iass2024.org/files/IASS_2024_Paper_341.pdf

6.3 Conference presentations

- Pool-Blanco SJ, “Obtención de coeficientes de presión en una estructura de membrana en condición cerrada y abierta”, presented at the *3^a Reunión Regional sobre Investigación en Ingeniería Estructural, Sociedad Mexicana de Ingeniería Estructural*, Mérida, Yucatán, México. 27th February 2019 (in Spanish).
- Pool Blanco SJ, “Computational wind engineering of an inflated membrane structure,” presented at the *18th Miklós Iványi International PhD & DLA Symposium*, Pécs, Hungary, 3-4 November 2022.
- Pool Blanco SJ, “Ingeniería eólica aplicada a estructuras de membrana” presented at the *II Congreso de Ciencias Exactas e Ingenierías (ConCEI-2)*, Mérida, Yucatán, México. 9-11 October 2024. (in Spanish).
- Pool Blanco SJ, “Ingeniería eólica aplicada a tenso estructuras” presented at the *II Congreso Interdisciplinario en Ciencias y Humanidades*, Chetumal, Quintana Roo, México. October 2024. (in Spanish).

References

- [1] W. Lewis, *Tension Structures: Form and behaviour*, 2 ed., London: ICE publishing, 2018.
- [2] E. Oñate and B. Kröplin, *Textile Composites and Inflatable Structures*, Dordrecht: Springer Dordrecht, 2005.
- [3] M. Seidel, *Tensile surface structures: A practical guide to cable and membrane construction*, Berlin: Ernst & Sohn, A Wiley Company, 2009.
- [4] A. L. Marbaniang, S. Ghosh and S. Dutta, "Tensile membrane structures: An overview," in *Advances in Structural Engineering, Lecture Notes in Civil Engineering*, vol. 74, 2020, pp. 29-40.
- [5] F. Fu, "Chapter Seven: Design and Analysis of Tensile Structures and Tensegrity Structures," in *Design and Analysis of Tall and Complex Structures*, Butterworth-Heinemann, 2018, pp. 213-249.
- [6] B. Kröplin, "Inflated membrane structures on the ground, in the air and in space-A classification," in *Textile Composites and Inflatable Structures*, vol. 3, Springer, 2005, pp. 213-220.
- [7] K. Hincz and M. Gamboa-Marrufo, "Deformed shape wind analysis of tensile membrane structures," *ASCE Journal of Structural Engineering*, vol. 142, no. 3, pp. 04015153-1-5, 2015.
- [8] C. Geurts and C. van Bentum, "Wind loading on buildings: Eurocode and experimental approach," in *Wind effects on buildings and design of wind-sensitive structures*, SpringerWien New York, 2007, pp. 31-65.
- [9] E. Simiu and H. Yeo, *Wind effects on structures: modern structural design for wind*, John Wiley & Sons Ltd, 2019.
- [10] K. Hincz, "Determination of the cutting pattern of prestressed tent structures," *Revista Portuguesa de Engenharia de Estruturas*, vol. 47, pp. 45-49, 2000.
- [11] J. Frank, C. Hirsch, A. G. Jensen, H. W. Krüs, M. Schatzmann, P. S. Westbury and et al., "Recommendations on the use of CFD in wind engineering," in *Proceedings of the International Conference on Urban Wind Engineering and Building Aerodynamics*, 2004.
- [12] J. Frank, A. Hellsten, H. Schlünzen and B. Carismo, *Best practice guideline for the CFD simulation of flows in the urban environment: COST action 732 quality assurance and improvement of microscale meteorological models*, COST Office, 2007.

- [13] T. Tamura, K. Nozawa and K. Kondo, "AIJ Guide for numerical prediction of wind loads on buildings," *Journal of Wind Engineering and Industrial Aerodynamics*, vol. 96, no. (10-11), pp. 1974-1984, 2008.
- [14] S. Pool-Blanco, . M. Gamboa-Marrufo, K. Hincz and C. Domínguez-Sandoval, "Wind tunnel tests of an inflated membrane structure. Two study cases: with and without end-walls," *Ingeniería Investigación y Tecnología*, vol. 23, no. 2, pp. 1-12, 2022.
- [15] A. S. Day, "An introduction to dynamic relaxation," *Engineer*, vol. 219, pp. 218-221, 1965.
- [16] B. H. V. Topping and P. Iványi, *Computer aided design of cable membrane structures*, Keppen, Stirlingshire, Scotland: Saxe-Coburg Publications, 2008.